Contents lists available at ScienceDirect

Colloids and Surfaces A: Physicochemical and Engineering Aspects
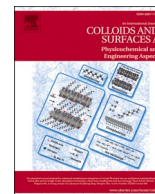
Multi-responsive self-assembly of polymeric-like building blocks nC$_{12}$C$_6$C$_{12}$(Me)@nγ-CD: Vesicles, nanotubes and sheet crystal

Zhijie Liu [a,b], Qiang Zhao [a], Shuitao Gao [a], Yun Yan [a], Baocai Xu [c,*], Cheng Ma [a,*], Jianbin Huang [a,*]

[a] Beijing National Laboratory for Molecular Sciences (BNLMS), State Key Laboratory for Structural Chemistry of Unstable and Stable Species, College of Chemistry and Molecular Engineering, Peking University, Beijing 100871, China
[b] School of Earth and Space Science, Peking University, Beijing 100871, China
[c] School of Food and Chemical Engineering, Beijing Technology and Business University, Beijing 100048, China

GRAPHICAL ABSTRACT
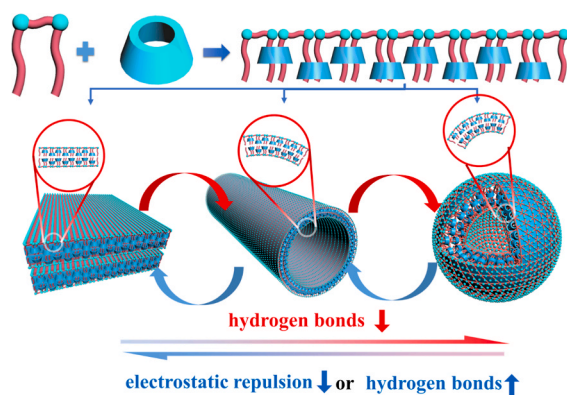
ARTICLE INFO

ABSTRACT

Surfactant@cyclodextrin (CD) inclusions regarded as specific building blocks can form a single unit with a 1:1 ratio through host-guest interaction, and self-assemble into various nanostructures in aqueous solution. In this study, a polymeric-like building block, nC$_{12}$C$_6$C$_{12}$(Me)@nγ-CD, is constructed by assembling e surfactant and γ-CD. This building block can assemble into well-defined nanostructures such as vesicles, nanotubes, and sheets in different concentrations. Due to the hydrogen bonding and electrostatic interactions to be the driving force of nC$_{12}$C$_6$C$_{12}$(Me)@nγ-CD aggregates formation, the morphologies among vesicles, nanotubes, and sheets could be reversibly transformed by multiple stimulus such as temperature, solvent additives, and ions.

* Corresponding authors.
  E-mail addresses: xubaoc@btbu.edu.cn (B. Xu), 1906392059@pku.edu.cn (C. Ma), JBHuang@pku.edu.cn (J. Huang).
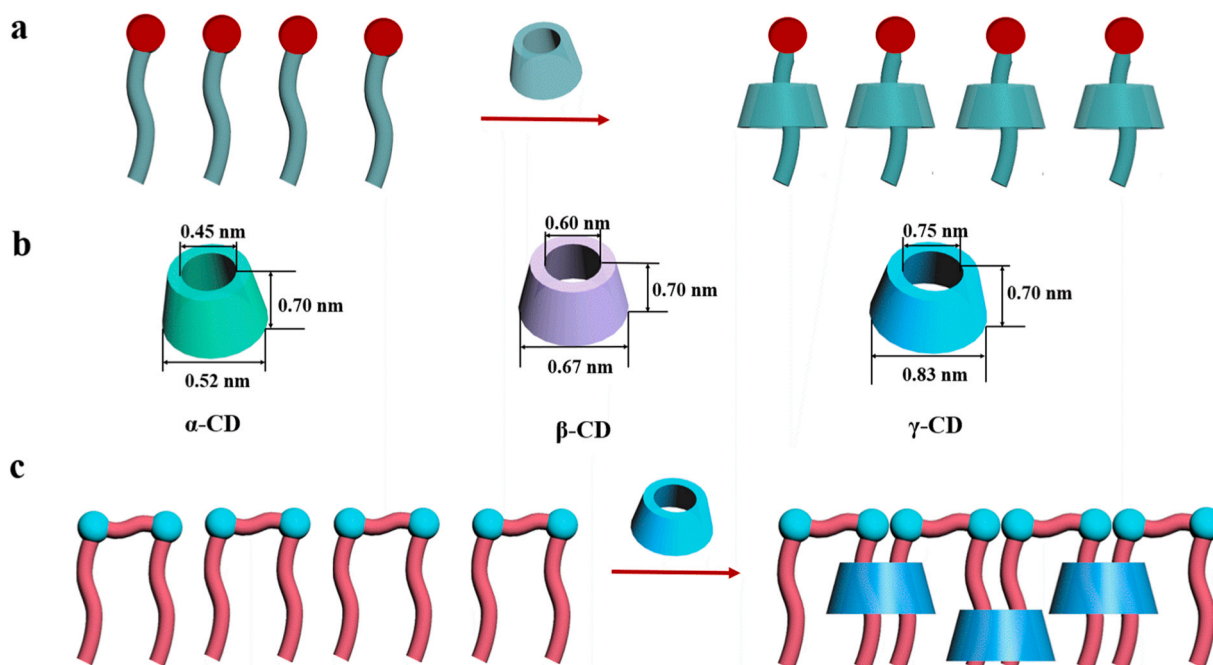
Scheme 1. (a) Schemes of surfactant@CD inclusions. (b) Structures and dimensions of different cyclodextrins. (c) Schemes of gemini surfactant@CD inclusions.

1. Introduction

Cyclodextrins (CDs) are oligosaccharide molecules that have a ring-like structure resembling a donut [1,2]. They have a hydrophilic outer surface that contains many hydroxyl groups, making them soluble in aqueous solutions. The inner cavity of CDs is hydrophobic and consists of glucoside methylene. As most surfactants are amphiphilic and have a hydrophobic tail, they can be inserted into the cavity of CDs, forming an inclusion structure in a 1:1 ratio through host-guest interactions (Scheme 1a) [3–10]. Previous studies have shown that surfactant@CD structures can break down or weaken surfactant aggregates by removing surfactants from the aggregation. For example, the addition of CDs can destroy micelles or air/water interface adsorption layers and increase the fluidity and permeability of liposomes [11]. However, the recent studies show that in concentrated solutions, these surfactant@CD inclusion complexes can be assembled into various nanostructures such as vesicles, microtubes, layers, and spirals through hydrogen bonding interactions with many hydroxyl groups on the outside of the CDs [12–18]. These results suggest that the surfactant@CD single unit could be an excellent building block for creating well-defined self-assemblies [19–22].

The dimension of cyclodextrins varies depending on the number of glucose molecules (Scheme 1b) [23–25]. α-CD is made up of 6 glucose molecules and has a cavity diameter of 0.45 nm. Meanwhile, β-CD is made up of 7 glucose molecules and has a cavity diameter of 0.60 nm, while γ-CD is made up of 8 glucose molecules and has a cavity diameter of 0.75 nm. Typically, α-CD and β-CD are used to fabricate inclusions with surfactants through host-guest interactions because the width of the surfactant is around 0.31 nm and could fit the cavity of α-CD and β-CD well. Different with them, it has been reported that γ-CD can accommodate two alkyl chains and form a binding ratio of 1:2 with a single surfactant [26,27]. Notably, gemini surfactants are specific molecules that have at least two alkyl chains and can form inclusions with γ-CD in diluted solutions [28–30]. However, to our best of knowledge, there is no report on gemini surfactant@CD inclusions that can form various nanostructures in concentrated solutions.

In our study, we present a polymeric-like inclusion based on the gemini surfactant $C_{12}C_6C_{12}$(Me) (N, N′-didodecyl-N, N, N′, N′-tetra-methyl-N, N′-hexamethylenediamine) and γ-CD (Scheme 1c), which is

shown to exhibit various structures such as vesicles, nanotubes, and sheets in aqueous solutions with increasing concentrations. Furthermore, the morphologies of $C_{12}C_6C_{12}$(Me)@ γ-CD aggregates can respond to multiple stimuli such as temperature, solvent additives, and ions, making the process reversible and possessing a promising potential for drug release applications in the future. The structure of the inclusion is systematically investigated through a set of methods, including isothermal titration microcalorimetry, 1 H-nuclear magnetic resonance (1 H NMR) measurements, electrospray ionization mass spectrometry, and atomic force microscopy. This study also provides a deeper understanding of the self-assembly mechanisms of surfactant@CD inclusion in concentrated solutions.

2. Experimental section

2.1. Materials

The cationic gemini surfactants N, N′-didodecyl-N, N, N′, N′-tetra-methyl-N, N′-hexamethylenediamine, which are abbreviated as $C_{12}C_6C_{12}$(Me), were synthesized and purified using methods found in previous literature[31]. The γ-cyclodextrin (γ-CD), urea and glucose were purchased from Macklin. Sodium chloride(NaCl) was purchased from Aladdin. The reagents used were of analytical grade. Ultrapure water was used throughout the entirety of the experiment.

2.2. Sample preparation

The desired amounts of $C_{12}C_6C_{12}$(Me) were added into the γ-CD solutions and then the samples were stirred and heated to be transparent. Then the solutions were incubated at 25 °C for 24 h. The investigated ratio of $C_{12}C_6C_{12}$(Me)/γ-CD ranged from 0.5 to 1.5, and the concentration of γ-CD covered a board range from 10 mmol/L to 50 mmol/L.

2.3. TEM observations

The structure of the self-assemblies was examined utilizing TEM (FEI Tecnai G2 T20, 120 kV, together with energy-dispersive spectroscopy measurement). The sample was deposited onto copper grids of 230 mesh
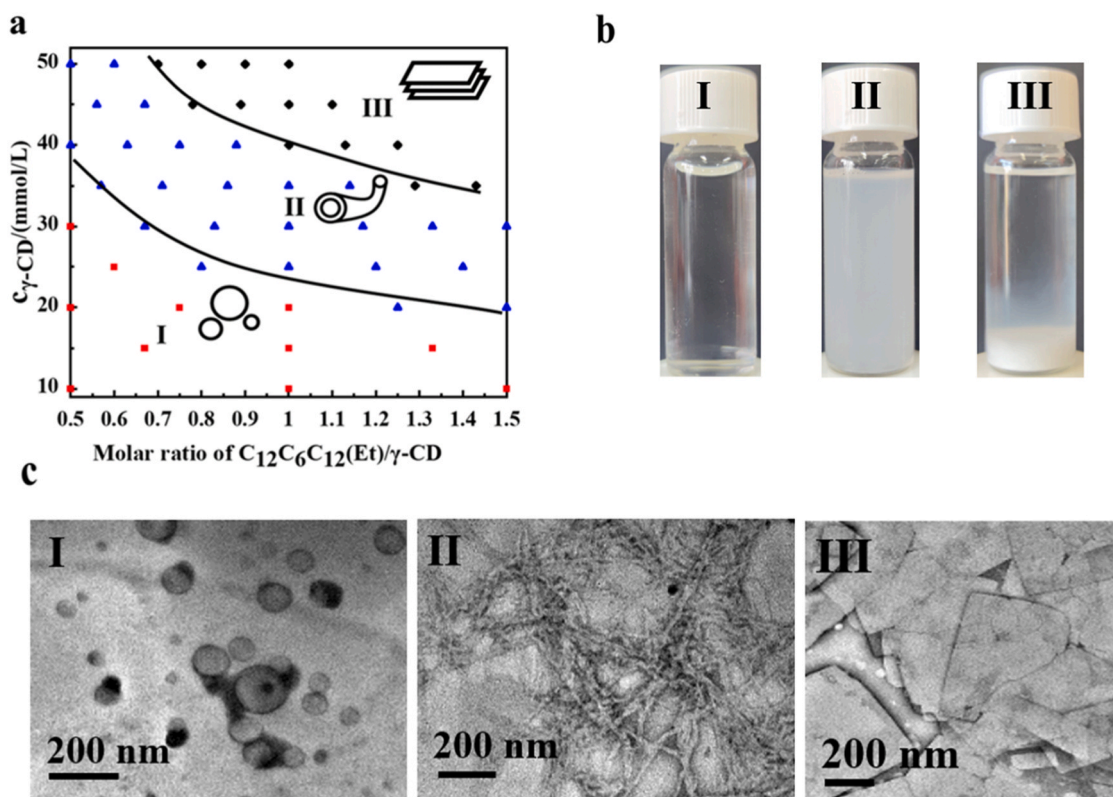
Fig. 1. (a) A phase diagram of $C_{12}C_6C_{12}(Me)/\gamma$-CD system. (b) Photographs of three samples in different regions, where the ratio of $C_{12}C_6C_{12}(Me)/\gamma$-CD is 1.0 for all the three samples and γ-CD concentration are 15 mmol/L (in region I), 30 mmol/L (in region II), 50 mmol/L (in region III). (c) TEM photographs of three samples in different regions.

that were coated with Formvar film, and any additional liquid was wiped away using filter paper. Negative staining with uranyl acetate was performed to enhance the contrast of the sample. The excess staining liquid was subsequently removed, and the samples were left to dry at room temperature in preparation for TEM analysis.

2.4. Atomic force microscopy (AFM)

The study utilized an Atomic Force Microscope (AFM) model D3100 (VEECO, USA) to perform measurements in tapping mode, under ambient conditions. To prepare the sample for analysis, a mixed aqueous solution was spin-coated onto a silicon substrate. The substrate was then cleaned using absolute ethanol and dried using N_2 flow through an ultrasonic process. The sample-loaded substrate was left to dry at room temperature before the AFM observation was conducted.

2.5. Nuclear magnetic resonance (NMR) studies

The lyophilized $C_{12}C_6C_{12}(Me)/\gamma$-CD precipitates were dissolved into DMSO-d6 for 1 H NMR and ^{2}D NMR (ROESY) measurements to determine the actual ratio of $C_{12}C_6C_{12}(Me)$ to γ-CD. The measurements were performed on an AVANCE III 500 MHz NMR (Bruker, Switzerland). All the proton signals were calibrated with the TMS at 0.00 ppm. By comparing the integration between γ-CD (H1 protons, d 4.83 ppm) and the total proton integration of $C_{12}C_6C_{12}(Me)$, the $C_{12}C_6C_{12}(Me)/\gamma$-CD complex ratio can be determined.

2.6. ESI-MS measurements

ESI-MS measurements were carried out on an APEX IV FT-MS (Bruker, USA). The ESI source was operated under positive ion mode with the following settings: spray voltage of 3300 V, capillary voltage of

3800 V, capillary temperature of 230 ℃, skimmer1 voltage of 33.0 V, skimmer2 voltage of 28.0 V, and sheath gas nitrogen pressure of 0.3 bar. To prepare the 1 mmol/L $C_{12}C_6C_{12}(Me)/\gamma$-CD vesicle samples for measurement, they were diluted 10 times with methanol and then directly infused into the ESI source at a flow rate of 3.00 mL/min.

2.7. Isothermal titration microcalorimetry (ITC)

An isothermal titration microcalorimeter, specifically the TAM 2277–201 model (Thermometric AB, J ̈arf ̈alla, Sweden) was employed to measure the enthalpy change. The microcalorimeter was equipped with a 1 mL sample cell made of stainless steel. Initially, the sample cell was loaded with 600 mL of either water or $C_{12}C_6C_{12}(Me)$ solution ($C_{C12C6C12}(Me) = 0.5$ mmol/L). Then, 2 mmol/L γ-CD solution was injected into the sample cell in portions of 10 mL using a 500 mL Hamilton syringe, which was controlled by a Thermometric 612 Lund pump. The system was stirred continuously with a gold propeller at 60 rpm until the desired concentration range was covered. The interval between injections was long enough to allow the signal to return to the baseline. The observed enthalpies (DHobs) were determined by integrating the areas of the peaks in the plot of thermal power against time. The reproducibility of the experiments was within 4 %. All measurements were conducted at a temperature of 25 ℃.

3. Results and discussion

3.1. Phase behavior and nanostructures of $C_{12}C_6C_{12}(Me)/\gamma$-CD system

The phase behavior and nanostructures of the $C_{12}C_6C_{12}(Me)/\gamma$-CD system were thoroughly investigated in this study. As shown in Fig. 1a, the system was divided into three regions, where in Region I, the solutions were clear and transparent (Fig. 1b, I), and the nanostructures
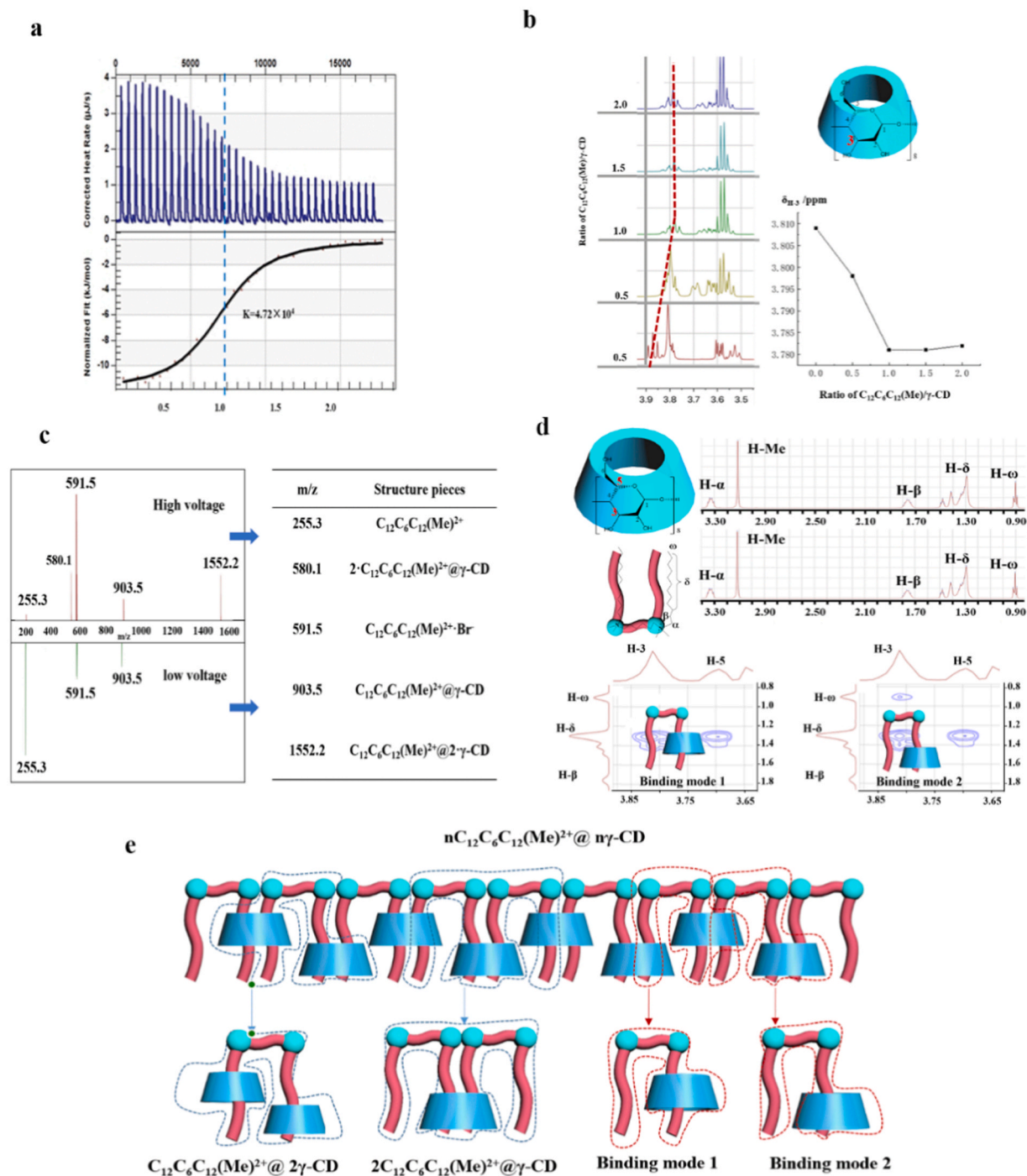
Fig. 2. (a) Calorimetric titration plot and normalized fitting curve of ITC, Titrant: 2.0 mmol/L γ-CD, titrand: 0.5 mmol/L $C_{12}C_6C_{12}(Me)$. (b) 1 H NMR spectra of $C_{12}C_6C_{12}(Me)$/γ-CD mixed system with the ratio of $C_{12}C_6C_{12}(Me)$/ γ-CD = 0.5, 1, 1.5, 2. (c) Mass spectra of $C_{12}C_6C_{12}(Me)$/γ-CD/water system under high voltage and low voltage. (d) ^{2}D NMR(ROESY) and structural scheme of $C_{12}C_6C_{12}(Me)$/γ-CD complex. (e) Scheme of the building block $nC_{12}C_6C_{12}(Me)@nγ$-CD in $C_{12}C_6C_{12}(Me)$/ γ-CD/water system.

observed were vesicles by means of transmission electron microscopy (TEM) (Fig. 1c, I). As the $C_{12}C_6C_{12}(Me)$/γ-CD ratio or γ-CD concentration increased, the solution became opalescent (Fig. 1b, II). Tube-like nanostructures appeared and co-existed with vesicles. And eventually, all vesicles disappeared, with only nanotubes left in Region II (Fig. 1c, II). At the same time, the diameters of nanostructures also changed with the increasement of concentration (Fig. S1). In Region III, precipitates with sheet structures were prevalent, as shown in Fig. 1b, III, and Fig. 1c, III. The nanostructures of the supernatant were similar to those in Region II, containing nanotubes and vesicles simultaneously. Overall, the

transformation of the nanostructures inside the system progressed from vesicles, to nanotubes, and ultimately to sheets with increasing $C_{12}C_6C_{12}(Me)$/γ-CD ratio or γ-CD concentration. In addition, it should be mentioned that the solutions of $C_{12}C_6C_{12}(Me)$ at different concentrations without addition of γ-CD were clear and transparent, and their morphology of the aggregates at the same concentration were spherical micelles[32].
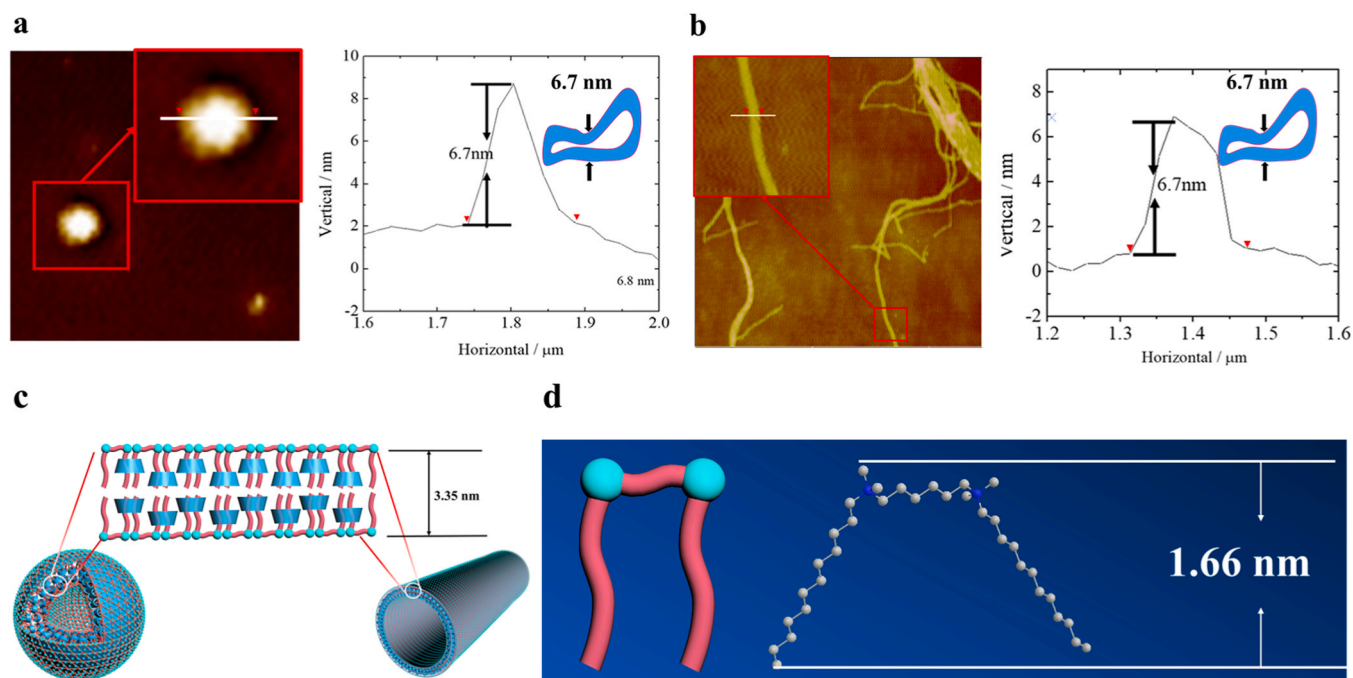
Fig. 3. AFM results of nanotubes (a) and vesicles (b) in $C_{12}C_6C_{12}(Me)@$ γ-CD system. (c) Scheme of molecular arrangement in nanotubes and vesicles. (d) Chem3D model of $C_{12}C_6C_{12}(Me)$.

3.2. Formation of $C_{12}C_6C_{12}(Me)/$γ-CD nanostructures

To investigate the formation of $C_{12}C_6C_{12}(Me)@$γ-CD inclusions driven by the host-guest interaction, and to determine the stoichiometric ratio of γ-CD and $C_{12}C_6C_{12}(Me)$ in the complex, several analytical techniques, including ITC, 1H NMR, ESI-MS, and AFM were conducted. As depicted in Fig. 2a, the calorimetric titration plot and normalized fitting curve demonstrated that the ratio of γ-CD and $C_{12}C_6C_{12}(Me)$ in the inclusion complex was 1:1 with a K value of 4.72×10^4. In the 1 H NMR spectra (Fig. 2b), the chemical shift for H-3 protons of γ-CD shifted to a higher field when it bounded with $C_{12}C_6C_{12}(Me)$, and reached a minimum value when the $C_{C12C6C12(Me)}$: $C_{γ-CD}$ ratio was 1:1, consistent with the result of ITC, both conforming the 1:1 ratio of $C_{12}C_6C_{12}(Me)/$γ-CD in the inclusion complex. ESI-MS analysis provided more detailed information on the nanostructures in aggregation under high and low voltages. As illustrated in Fig. 2c, the pieces of aggregates were shown with different m/z peaks and calculated with different types of inclusions. The pieces of $C_{12}C_6C_{12}(Me)@$γ-CD included 2:1, 1:1 and 1:2 ratios, denoted as $2 \cdot C_{12}C_6C_{12}(Me)@$γ-CD, $C_{12}C_6C_{12}(Me)@$γ-CD, and $C_{12}C_6C_{12}(Me)@2 \cdot$γ-CD. However, the pieces of $2 \cdot C_{12}C_6C_{12}(Me)@$γ-CD and $C_{12}C_6C_{12}(Me)@2 \cdot$γ-CD were unstable, because it was not shown in the result of ESI-MS under low voltages. Notably, different from our previous research that surfactants co-assembly with cyclodextrins usually forming inclusions with a single unit, in this work, our finding showed that gemini surfactants probably led to a polymeric-like nanostructure through host-guest interaction, where the cyclodextrins were regarded as the cross-linker to bind the two neighbor units together with different types of inclusions, thus resembling a polymeric-like chains.

The position and orientation of γ-CD outside $C_{12}C_6C_{12}(Me)$ in the polymeric-like $nC_{12}C_6C_{12}(Me)@$nγ-CD unit were further determined by means of ^{2}D NMR. As illustrated in Fig. 2d, the H-3 and H-5 of γ-CD were found to be located in the up and bottom sides, respectively. Meanwhile, the H-β, H-δ, and H-ω of $C_{12}C_6C_{12}(Me)$ indicated that the H position from head to tail. Two types of correlations were detected by ^{2}D NMR, suggesting that γ-CDs were in two positions along $C_{12}C_6C_{12}(Me)$'s alkyl chain. The correlation between H-3 and H-ω, H-5 and H-δ confirmed that some γ-CDs were in a bottom-up orientation and located outside the tail

of $C_{12}C_6C_{12}(Me)$'s alkyl chain. Similarly, the correlation between H-3 and H-δ, H-5 and H-δ verified that other γ-CDs were in the middle of $C_{12}C_6C_{12}(Me)$'s alkyl chain with the same bottom-up direction. An overview of the inclusive structure between γ-CD and $C_{12}C_6C_{12}(Me)$ was provided in Fig. 2e, where the different locations of γ-CDs may result from the large dimension of γ-CD leading to a steric effect. This polymeric-like unit constructed by γ-CD and $C_{12}C_6C_{12}(Me)$ further self-assembled into aggregates, such as vesicles, nanotubes, or sheets in different ratios or concentrations through the hydrogen bonds.

Next, AFM measurements were conducted on both vesicles and nanotubes to determine the arrangement of the $nC_{12}C_6C_{12}(Me)@$nγ-CD building blocks in the aggregates. As shown in Fig. 3a, the height of the collapsed vesicle was measured to be approximately 6.7 nm, which was indicative of a bilayer structure. Similarly, the nanotube, was also confirmed to exhibit a bilayer structure with a height of approximately 6.7 nm (Fig. 3b). The width of the nanotube was approximately 200 nm, which was larger than the dimension observed by TEM (50–100 nm). This difference may be attributed to the broadening effect of AFM tips during measurement. The height of approximately 6.7 nm was also observed in both vesicles and nanotubes, indicating that the building blocks of $nC_{12}C_6C_{12}(Me)@$nγ-CD constructed a double-layer structure in the aggregation process (Fig. 3c). This suggested that both vesicles and nanotubes were formed through a similar process, with the building blocks arranged in a bilayer structure. The height of $C_{12}C_6C_{12}(Me)$ single layer is about 1.66 nm according to Chem3D calculation as shown in Fig. 3d.

3.3. Multiple responses of $C_{12}C_6C_{12}(Me)@$γ-CD aggregates in aqueous solution

The formation of vesicles was investigated with regards to non-covalent interactions. It is well established that the main driving force between surfactant@CD building blocks in aggregates is hydrogen bonding [33]. Similarly, the formation of $nC_{12}C_6C_{12}(Me)@$nγ-CD aggregates was found to be driven by hydrogen bonding and electrostatic interactions, which could exhibit multiple responses to temperature, additives, and ions. First, it is observed that temperature played a crucial
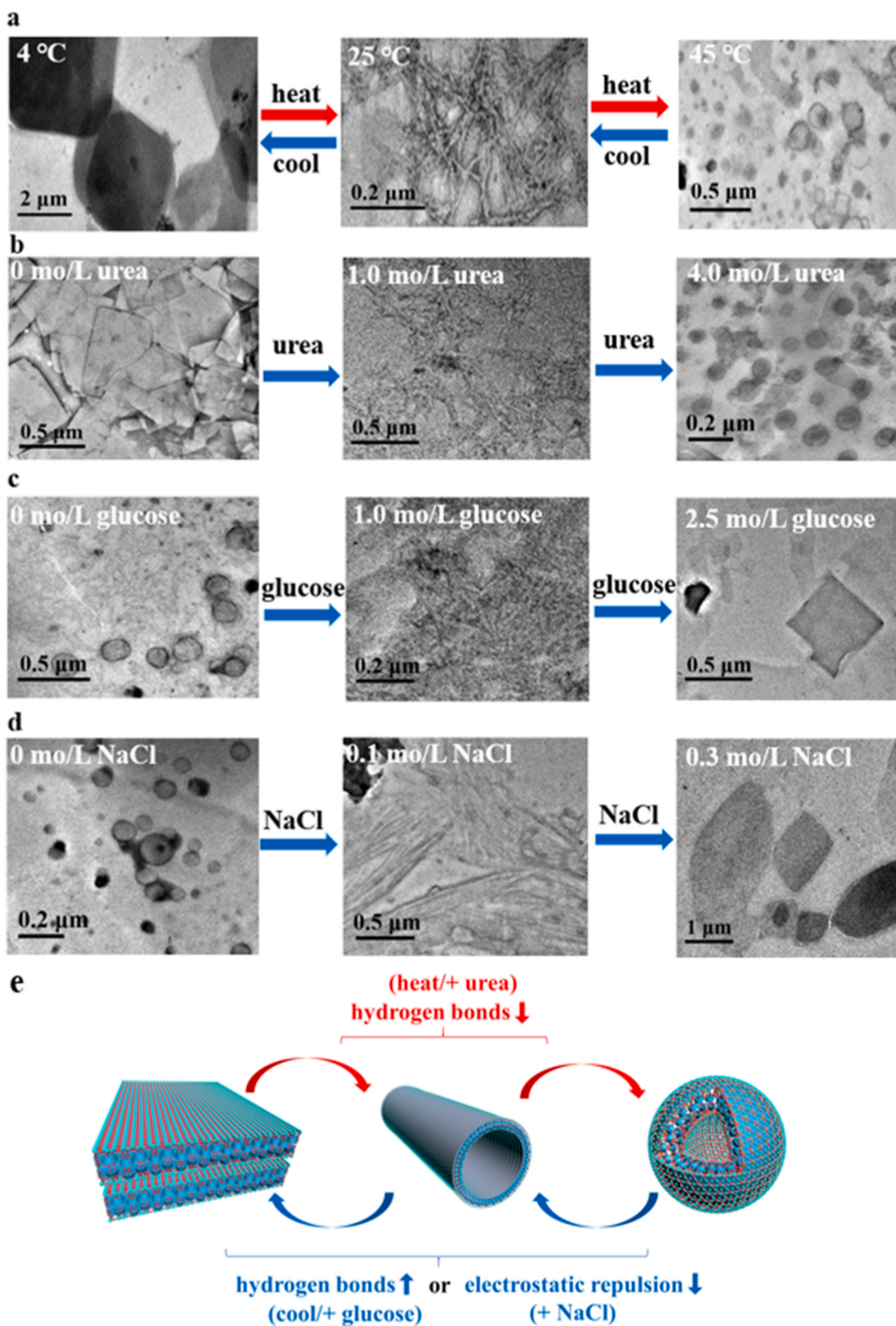
Fig. 4. Aggregation behaviors of $C_{12}C_6C_{12}(Me)/\gamma$-CD system: (a) TEM images of the sample at 4 ℃, 25 ℃, and 45 ℃, ($C_{\gamma\text{-CD}}$ = 30 mmol/L, $C_{C12C6C12(Me)}$ = 30 mmol/L). (b) TEM images of the sample with 0, 1.0 and 4.0 mol/L urea, ($C_{\gamma\text{-CD}}$ = 50 mmol/L, $C_{C12C6C12(Me)}$ = 50 mmol/L). (c) TEM images of the sample with 0, 1.0 and 2.5 mol/L glucose, ($C_{\gamma\text{-CD}}$ = 20 mmol/L, $C_{C12C6C12(Me)}$ = 20 mmol/L). (d) TEM images of the sample with 0, 0.1 and 0.3 mol/L NaCl, ($C_{\gamma\text{-CD}}$ = 20 mmol/L, $C_{C12C6C12(Me)}$ = 20 mmol/L). (e) Scheme of multiple responses of $C_{12}C_6C_{12}(Me)@\gamma$-CD aggregates behavior.

role in determining the nanostructure formation of the system. As shown in Fig. 4a, at temperatures below 4 ℃, sheets were the primary aggregates in the γ-CD/$C_{12}C_6C_{12}$(Me) system. When the temperature was increased to 25 ℃, the sheets transformed into nanotubes. Upon further heating to above 45 ℃, the aggregates varied from nanotubes to vesicles. Furthermore, the temperature-induced transitions were reversible. This was because higher temperature intensified molecular thermos motion, which reduced the formation of hydrogen bonds between γ-CD/$C_{12}C_6C_{12}$(Me) building blocks, thus resulting in smaller dimensions of the aggregates and more soluble physical behavior.

Next, it is observed that urea and glucose, which are common additives in aqueous solution to decrease and increase the formation of intermolecular hydrogen bonding [34,35], could also make n$C_{12}C_6C_{12}$(Me)@nγ-CD aggregates a revisable transformation. As shown in Fig. 4b, after the addition of 1 mol/L and 4 mol/L urea, the sheets turned into nanotubes and vesicles, respectively. It should be noted that when adding 1.0 mol/L and 2.5 mol/L glucose to vesicles solution, the whole process was reversible (Fig. 4c). Besides hydrogen bonds between γ-CDs, the electrostatic repulsions of head groups among $C_{12}C_6C_{12}$(Me)s also influenced the formation of aggregates. In this context, electrostatic repulsions between building blocks shielded by addition of NaCl will lead to morphological change of the aggregates. As shown in Fig. 4d, as the concentration of NaCl increased, the aggregates varied from vesicles, to nanotubes then sheets. Furthermore, the changes of aggregate structure affected the turbidity of the solutions. As shown in Fig. S2, the absorbance of the solutions could be reversibly transformed by multiple stimuli, such as temperature, solvent additives, and ions. Overall, it was demonstrated that morphologies n$C_{12}C_6C_{12}$(Me)@nγ-CD aggregates among vesicles, nanotubes, and sheets can be reversibly transformed by multiple stimulus such as temperature, solvent additives, and ions. And the morphological changes of aggregates could be attributed to increasing or decreasing the formation of intermolecular hydrogen bonding between γ-CDs, and shielding electrostatic repulsions of head groups among $C_{12}C_6C_{12}$(Me)s, respectively (Fig. 4e). More importantly, the multi-responsive properties are expected to hold a potential application in drug release or other smart applications in the future.

4. Conclusion

In conclusion, a multi-responsive self-assembly soft matter derived from $C_{12}C_6C_{12}$(Me)@γ-CD was successfully fabricated in aqueous solutions. The morphology of the aggregates could transform from vesicles to nanotubes and sheets in different concentrations, with a consistent polymeric-like n$C_{12}C_6C_{12}$(Me)@nγ-CD building block. Hydrogen bonds and electrostatic interactions were identified as the driving force for the self-assembly. The morphologies of the aggregates could be reversibly transformed by multiple stimuli, such as temperature, solvent additives, and ions. For further research, the polymeric-like building block of surfactant@cyclodextrin inclusions would aid in the construction of novel nanostructures, and benefit the fundamental research on supramolecular assembly mechanisms. It is also envisioned that polymeric-like building block will have unique advantages and broad application prospects in the fabrication of stimulus-responsive materials, self-healing materials, and biomedical materials.

CRediT authorship contribution statement

Zhijie Liu: Methodology, Formal analysis, Investigation, Resources, Data curation, Visualization, Writing – original draft. **Qiang Zhao**: Conceptualization, Methodology, Formal analysis. **Shuitao Gao**: Writing – review & editing. **Yun Yan**: Writing – review & editing, Supervision. **Baocai Xu**: Writing – review & editing, Supervision. **Cheng Ma**: Methodology, Resources, Writing – review & editing, Supervision. **Jianbin Huang**: Writing – review & editing, Supervision, Funding acquisition.

Declaration of Competing Interest

The authors declare that they have no known competing financial interests or personal relationships that could have appeared to influence the work reported in this paper.

Data Availability

Data will be made available on request.

Appendix A. Supporting information

Supplementary data associated with this article can be found in the online version at doi:10.1016/j.colsurfa.2023.132269.

References

[1] A. Harada, J. Li, M. Kamachi, The molecular necklace: a rotaxane containing many threaded α-cyclodextrins, Nature 356 (1992) 325–327.
[2] M.V. Rekharsky, Y. Inoue, Complexation thermodynamics of cyclodextrins, Chem. Rev. 98 (1998) 1875–1918.
[3] A.B. Dorrego, L. Garcia-Rio, P. Herves, J.R. Leis, J.C. Mejuto, J. Perez-Juste, Micellization versus cyclodextrin–surfactant complexation, Angew. Chem. Int. Ed. 39 (2000) 2945–2948.
[4] J.W. Park, H.J. Song, Association of anionic surfactants with.beta.-cyclodextrin: fluorescence-probed studies on the 1:1 and 1:2 complexation, J. Phys. Chem. 93 (1989) 6454–6458.
[5] V.I. Martín, P. López-Cornejo, M. López-López, D. Blanco-Arévalo, A.J. Moreno-Vargas, M. Angulo, A. Laschewsky, M.L. Moyá, Influence of the surfactant degree of oligomerization on the formation of cyclodextrin: surfactant inclusion complexes, Arab. J. Chem. 13 (2020) 2318–2330.
[6] U.R. Dharmawardana, S.D. Christian, E.E. Tucker, R.W. Taylor, J.F. Scamehorn, A surface tension method for determining binding constants for cyclodextrin inclusion complexes of ionic surfactants, Langmuir 9 (1993) 2258–2263.
[7] L.X. Jiang, M.L. Deng, Y.L. Wang, Y. Yan, J.B. Huang, Special effect of β-Cyclodextrin on the aggregation behavior of mixed cationic/anionic surfactant systems, J. Phys. Chem. B 113 (2009) 7498–7504.
[8] N. Li, L. Yun, X. Ji, S. Mukherjee, C. Wang, Y. Chen, Construction of photoresponsive azobenzene-decorated cationic surfactant-based self-assembled vesicles and controlled drug release, Colloid Surf. A 631 (2021), 127711.
[9] L.X. Jiang, C.F. Yu, M.L. Deng, C.W. Jin, Y.L. Wang, Y. Yan, J.B. Huang, Selectivity and stoichiometry boosting of β-Cyclodextrin in cationic/anionic surfactant systems: when host-guest equilibrium meets biased aggregation equilibrium, J. Phys. Chem. B 114 (2010) 2165–2174.
[10] L.S. Hao, H.X. Wang, Y.S. Wang, Y.Q. Meng, Y.Q. Nan, Inclusion complexation of surfactant with β-cyclodextrin and its effect on the mixed micellization of cationic/anionic surfactants, Colloid Surf. A 668 (2023), 131437.
[11] L.X. Jiang, Y. Yan, J.B. Huang, Versatility of cyclodextrins in self-assembly systems of amphiphiles, Adv. Colloid Interface Sci. 169 (2011) 13–25.
[12] L.X. Jiang, Y. Peng, Y. Yan, M.L. Deng, Y.L. Wang, J.B. Huang, "Annular ring" microtubes formed by SDS@2β-CD complexes in aqueous solution, Soft Matter 6 (2010) 1731–1736.
[13] L.X. Jiang, Y. Yan, J.B. Huang, Zwitterionic surfactant/cyclodextrin hydrogel: microtubes and multiple responses, Soft Matter 7 (2011) 10417–10423.
[14] L.X. Jiang, Y. Peng, Y. Yan, J.B. Huang, Aqueous self-assembly of SDS@2β-CD complexes: lamellae and vesicles, Soft Matter 7 (2011) 1726–1731.
[15] X.J. Wang, X.D. Gao, X. Xiao, S.S. Jiang, Y. Yan, J.B. Huang, Photoresponsive supramolecular strategy for controlled assembly in light-inert double-chain surfactant system, J. Colloid Interface Sci. 594 (2021) 727–736.
[16] C.C. Zhou, X.H. Cheng, Q. Zhao, Y. Yan, J.D. Wang, J.B. Huang, Self-assembly of nonionic surfactant tween 20@2β-CD inclusion complexes in dilute Solution, Langmuir 29 (2013) 13175–13182.
[17] C.C. Zhou, X.H. Cheng, Q. Zhao, Y. Yan, J.D. Wang, J.B. Huang, Self-assembly of channel type β-CD dimers induced by dodecane, Sci. Rep. 4 (2014) 7533.
[18] S.Y. Yang, Y. Yan, J.B. Huang, A. Petukhov, Loes M.J. Kroon-Batenburg, Markus Drechsler, C.C. Zhou, M. Tu, S. Granick, L.X. Jiang, Giant capsids from lattice self-assembly of cyclodextrin complexes, Nat. Commun. 8 (2017) 15856.
[19] X.J. Wang, W.W. Zhi, C. Ma, Z.Y. Zhu, W.L. Qi, J.B. Huang, Y. Yan, Not by serendipity: rationally designed reversible temperature-responsive circularly polarized luminescence inversion by coupling two scenarios of Harata−Kodaka's rule, JACS Au 1 (2021) 156–163.
[20] X. Xiao, Z.R. Xu, W.K. Wang, S.Y. Sun, Y. Qiao, L.X. Jiang, Y. Yan, J.B. Huang, Enzyme-responsive molecular assemblies based on host−guest chemistry, Langmuir 37 (2021) 8348–8355.

[21] X. Li, M. Porcino, C. Martineau-Corcos, T. Guo, T. Xiong, W.F. Zhu, G. Patriarche, C. Pechoux, B. Perronne, A. Hassan, R. Kummerle, A. Michelet, A. Zehnacker-Rentien, J.W. Zhang, R. Gref, Efficient incorporation and protection of lansoprazole in cyclodextrin metal-organic frameworks, Int. J. Pharm. 585 (2020), 119442.

[22] X.J. Wang, Y.T. Liu, T.Y. Wu, B.F. Gu, H. Sun, H.L. He, H.Q. Gong, H. Zhu, A win-win scenario for antibacterial activity and skin mildness of cationic surfactants based on the modulation of host-guest supramolecular conformation, Bioorg. Chem. 134 (2023), 106448.

[23] P. Brocos, N. Diaz-Vergara, X. Banquy, S. Perez-Casas, M. Costas, A. Pineiro, Similarities and differences between cyclodextrin-sodium dodecyl sulfate host-guest complexes of different stoichiometries: molecular dynamics simulations at several temperatures, J. Phys. Chem. B 114 (2010) 12455–12467.

[24] L. dos Santos Silva Araújo, G. Lazzara, L. Chiappisi, Cyclodextrin/surfactant inclusion complexes: an integrated view of their thermodynamic and structural properties, Adv. Colloid Interface Sci. 289 (2021), 102375.

[25] A.A. Sandilya, U. Natarajan, M.H. Priya, Molecular view into the cyclodextrin cavity: structure and hydration, ACS Omega 5 (2020) 25655–25667.

[26] T. Ogoshi, K. Masuda, T. Yamagishi, Y. Nakamoto, Side-Chain polypseudorotaxanes with heteromacrocyclic Receptors of cyclodextrins (CDs) and cucurbit[7]uril (CB7): their contrast lower critical solution temperature behavior with α-CD, γ-CD, and CB7, Macromolecules 42 (2009) 8003–8005.

[27] X.K. Qu, L.Y. Zhu, L. Li, X.L. Wei, F. Liu, D.Z. Sun, Host-guest complexation of β-, γ-cyclodextrin with alkyl trimethyl ammonium bromides in aqueous solution, J. Solut. Chem.. 36 (2007) 643–650.

[28] F.M. Menger, J.S. Keiper, Gemini surfactants, Angew. Chem. Int. Ed. 39 (11) (2000) 1906–1920.

[29] M.W. Cao, M.L. Deng, X.L. Wang, Y.L. Wang, Decompaction of cationic gemini surfactant-induced DNA condensates by β-cyclodextrin or anionic surfactant, J. Phys. Chem. B 112 (2008) 13648–13654.

[30] W.T. Wang, Y.C. Han, J. Zhu, Y.X. Fan, Y.L. Wang, Seeded growth of gold nanoparticles in aqueous solution of cationic gemini surfactants with different spacer length: influences of molecular and aggregate structures, J. Nanopart. Res. 21 (2019) 24.

[31] R. Zana, M. Benrraou, R. Rueff, Alkanediyl-α,ω-bis-(dimethylalkylammonium bromide) surfactants. 1. Effect of the spacer chain length on the critical micelle concentration and micelle ionization degree, Langmuir 7 (1991) 1072–1075.

[32] D. Danino, Y. Talmon, R. Zana, Alkanediyl-α, ω-bis(dimethylalkylammonium bromide) surfactants (dimeric surfactants). 5. Aggregation and microstructure in aqueous solutions, Langmuir 11 (1995) 1448–1456.

[33] C.C. Zhou, X.H. Cheng, Y. Yan, J.D. Wang, J.B. Huang, Reversible transition between SDS@2β-CD microtubes and vesicles triggered by temperature, Langmuir 30 (2014) 3381–3386.

[34] H.S. Frank, F. Franks, Structural approach to the solvent power of water for hydrocarbons; urea as a structure breaker, J. Chem. Phys. 48 (1968) 4746–4757.

[35] I.G. Chudotvortsev, O.B. Yatsenko, Concentration and temperature of eutectic points in glucose-water and saccharose-water systems, determined by the method of fractional melting of ice, Russ. J. Appl. Chem. 80 (2007) 201–205.